Observation of non-Fermi liquid behavior in hole-doped $Eu_2Ir_2O_7$

A. Banerjee,[1] J. Sannigrahi,[2] S. Giri,[1] and S. Majumdar[1,*]

[1]*Department of Solid State Physics, Indian Association for the Cultivation of Science, 2A & B Raja S. C. Mullick Road, Jadavpur, Kolkata 700 032, India*

[2]*ISIS Neutron and Muon Source Science and Technology Facilities Council, Rutherford Appleton Laboratory, Didcot OX11 0QX, United Kingdom*

(Received 5 July 2017; revised manuscript received 5 September 2017; published 21 December 2017)

The Weyl semimetallic compound $Eu_2Ir_2O_7$ and its hole-doped derivatives (which are achieved by substituting trivalent Eu by divalent Sr) are investigated through transport, magnetic, and calorimetric studies. The metal-insulator transition (MIT) temperature is found to get substantially reduced with hole doping, and for 10% Sr doping the composition is metallic down to temperature as low as 5 K. These doped compositions are found to violate the Mott-Ioffe-Regel condition for minimum electrical conductivity and show a distinct signature of non-Fermi liquid behavior at low temperature. The MIT in the doped compounds does not correlate with the magnetic transition point, and Anderson-Mott-type disorder-induced localization may be attributed to the ground-state insulating phase. The observed non-Fermi liquid behavior can be understood on the basis of disorder-induced distribution of the spin-orbit-coupling parameter, which is markedly different in the case of Ir^{4+} and Ir^{5+} ions.

DOI: 10.1103/PhysRevB.96.224426

I. INTRODUCTION

Recently, the physics of iridium-based oxides have created considerable excitement due to their fascinating electronic and magnetic properties originating from the interplay between spin-orbit coupling (SOC), electron correlation U, and intersite charge hopping [1,2]. Because of the extended nature of the $5d$ orbitals of Ir, these materials are associated with wider electronic band W and relatively weaker U and are expected to be metallic in nature. However, due to the large atomic number of Ir, the relativistic SOC plays an important role (in fact, the energy scales of SOC and U are comparable in magnitude), which in tandem with U can lead to an insulating ground state. The classic example is the layered oxide Sr_2IrO_4 with Ir^{4+} ($5d^5$) [1], where SOC splits the t_{2g} level into two bands with pseudospins $J_{\text{eff}} = \frac{1}{2}$ doublet and $J_{\text{eff}} = \frac{3}{2}$ quadruplet and thereby effectively reduces the bandwidth [see Fig. 1(a)]. The higher occupied $J_{\text{eff}} = \frac{1}{2}$ band is half filled and can open up a Mott gap through electron correlation. However, the system can have a metallic ground state if the band width of the t_{2g} level is large [see Fig. 1(b)].

Apart from Sr_2IrO_4, the pyrochlore iridates $R_2Ir_2O_7$ (R = rare earth) are found to be quite intriguing materials for which the samples show a metal-insulator (MI) transition on cooling, leading to an insulating ground state [3,4]. Such a MI transition is expected to be associated with the interplay between SOC and electron correlations. For decades, rare-earth pyrochlores such as $Dy_2Ti_2O_7$ and $Ho_2Ti_2O_7$ have attracted considerable attention for their unique magnetic frustration of geometrical origin which leads to the spin-ice state and the formation of Dirac monopoles [5,6]. The pyrochlore iridates are also a correlated electron system showing magnetic frustration. Theoretical studies indicate that these compounds are good candidates for topological materials [7–9]. Very recently, Sushkov *et al.* identified $Eu_2Ir_2O_7$ as a Weyl semimetal from terahertz optical conductivity studies [10].

The MI transition temperature T_{MI} in $R_2Ir_2O_7$ varies monotonically with the ionic radius of the R atom [3,11]. T_{MI} also coincides with the magnetic transition temperature T_N of the compounds, and it is found to be second order in nature [11]. At T_N, they undergo a commensurate long-range order where Ir^{4+} moments form an *all-in-all-out* configuration with all the moments pointing either toward or outward with respect to the center of the tetrahedron formed by the Ir^{4+} ions [12–14]. Pesin and Balents [7] pointed out that the insulating ground state of these pyrochlores can be aptly described as a "topological Mott" insulating phase. Ueda *et al.* [15] observed a successive phase change of the ground state of $Nd_2Ir_2O_7$ on doping from a narrow-gap Mott insulator to a Weyl semimetal and, finally, to a correlated metal, which can be attributed to the mutual interplay of SOC and U.

Despite the wealth of theoretical and experimental works, the true nature of the MI transition and the insulating ground state of these pyrochlores is a matter of debate. It is clear that the electron occupancy in Ir plays an important role in the MI transition. In the present work we have performed a systematic study of hole doping in one such Ir pyrochlore, $Eu_2Ir_2O_7$, and carried out transport, magnetic, and calorimetric studies of the derived materials. Hole doping is expected to vary the Ir valency, and it may affect the Ir-O-Ir bond angle. Our study indicates a systematic lowering in T_{MI} of the samples with Sr substitution. A significant outcome of this work is the observation of a non-Fermi liquid ground state in certain samples, a phenomenon that was earlier predicted theoretically for topological states with strong SOC [16].

II. EXPERIMENTAL DETAILS

Hole doping in $Eu_2Ir_2O_7$ was realized by substituting Eu^{3+} by Sr^{2+}. The polycrystalline samples $Eu_{1-x}Sr_xIr_2O_7$ ($x = 0.0$, 0.1, 0.15 and 0.2) were prepared through the solid-state

*sspsm2@iacs.res.in

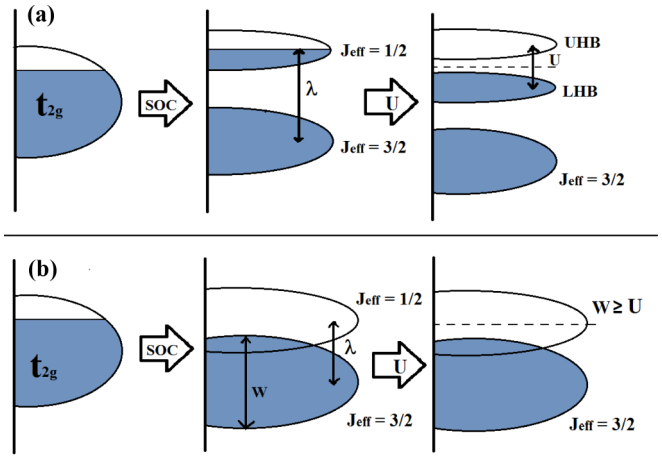

FIG. 1. (a) Schematic description of the splitting of the t_{2g} band of Ir 5*d* under SOC and U, leading to an insulating state where the completely filled lower Hubbard band (LHB) is separated from the empty upper Hubbard band (UHB) by an energy gap. (b) The case with large bandwidth ($W \gtrsim$ SOC, U), where overlapping bands can lead to a metallic state (see text).

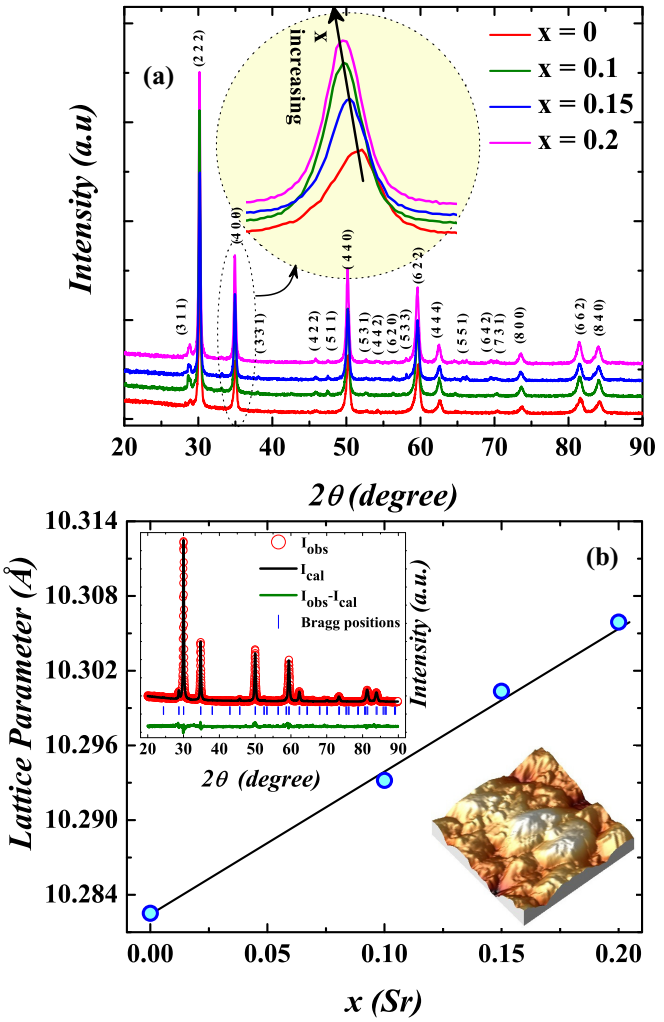

FIG. 2. (a) The powder x-ray diffraction pattern of $Eu_{1-x}Sr_xIr_2O_7$ ($x = 0.0$, 0.1, 0.15, and 0.2) samples recorded at room temperature. The inset shows the shift of the (400) reflection with doping. (b) The variation of the cubic lattice parameter as a function of doping concentration. The top inset shows the Rietveld refined data for the $x = 0.2$ sample, where the solid line is the fitted curve and the scattered points are the experimental data. The bottom inset shows the topograph of a flat surface of the $x = 0.0$ sample recorded by using an atomic force microscope.

reaction route. Stoichiometric amounts of Eu_2O_3, $SrCO_3$, and IrO_2 were mixed intimately and fired at 1223 K for 1 day. After the mixture powder was pressed into pellets, they were heated in air for 3 days at 1273 K with several intermediate grindings. The structure and phase purity of the samples were investigated by powder x-ray diffraction (XRD) using Cu K_α radiation. Detailed analysis confirms the cubic pyrochlore-type phase (space group $Fd\bar{3}m$) for all the samples, as depicted in Fig. 2(a). The peaks shift to a lower angle with increasing x, which is better viewed in the inset of Fig. 2(a). We have performed Rietveld refinement of the XRD data using the FULLPROF suite [17], and representative fitted data are shown for the $x = 0.2$ sample in the top inset of Fig. 2(b). The fitting for all the samples converges well, with χ^2 lying between ~2 and 1. The site occupancy of different atoms is found to be close to unity, indicating the absence of any substantial site vacancies. The cubic lattice parameter a_c shows almost linear variation with x following Vegard's law [Fig. 2(b)], which indicates that Sr is systematically getting substituted at the Eu site. In order to probe the grain and grain boundaries as well as any void in the sample, we studied the sample topography using atomic force microscope (Veeco-diCP II). A representative figure of a flat surface of an $x = 0.0$ pellet is shown in the bottom inset of Fig. 2(b). From the image, the grains are clearly visible, measuring about 100–300 nm. The grains are closely packed without any obvious void. Similar topography is also obtained for the other samples. The estimated mass density of the pellet of the $x = 0.0$ sample is about 7.3 (±10%) g/cm^3, which is about 75% of the x-ray density, and it is an indication of the compactness of the sample. The magnetic measurements were performed on a vibrating sample magnetometer from Cryogenic Ltd., as well as on a Quantum Design superconducting quantum interference device magnetometer. The zero-field and in-field resistivity ρ were measured using the four-probe method on a cryogen-free high-magnetic-field system (Cryogenic Ltd.) with magnetic field H as high as 50 kOe and within the temperature T range between 2 and 300 K. Heat capacity C_p measurement was carried out using a Quantum Design physical properties measurement system. The pure and $x = 0.2$ samples were also investigated through core-level x-ray photoelectron spectroscopy (XPS) at room temperature using Al K_α radiation on a laboratory-based commercial instrument (Omicron). The sample surfaces were cleaned *in situ* by argon ion sputtering. Figures 3(a) and 3(b) show the spin-orbit split Ir 4*f* core-level spectra for the $x = 0.0$ and 0.2 samples, respectively. The spectrum for the $x = 0.2$ sample shifts to higher binding energy, presumably due to the presence of Ir^{5+} states. The spectrum of the pure sample can be fitted with a single spin-orbit split doublet with a separation of 3.0 eV, while for the $x = 0.2$ sample two doublets are required to

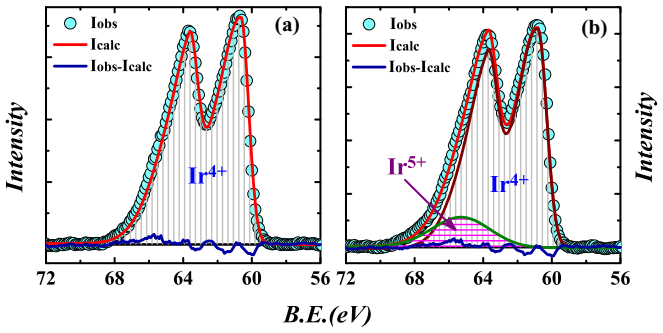

FIG. 3. (a) and (b) The $4f$ core-level XPS data for $x = 0.0$ and $x = 0.2$ samples, respectively. The solid lines are fit to the data with the model discussed in the text.

achieve good fitting. The additional weak doublet (marked with horizontal lines) occurring at a higher binding energy is likely to be connected to the minority Ir^{5+} ions [18], indicating the mixed valency in the Sr-doped sample.

III. RESULTS

Figures 4(a)–4(d) show the T dependence of magnetic susceptibility $\chi(T)$ $[=M(T)/H]$ for the $x = 0.0$, 0.1, 0.15, and 0.2 samples measured in zero-field-cooled (ZFC) and field-cooled (FC) protocols. For the parent sample, a magnetic anomaly is observed close to 120 K, below which there

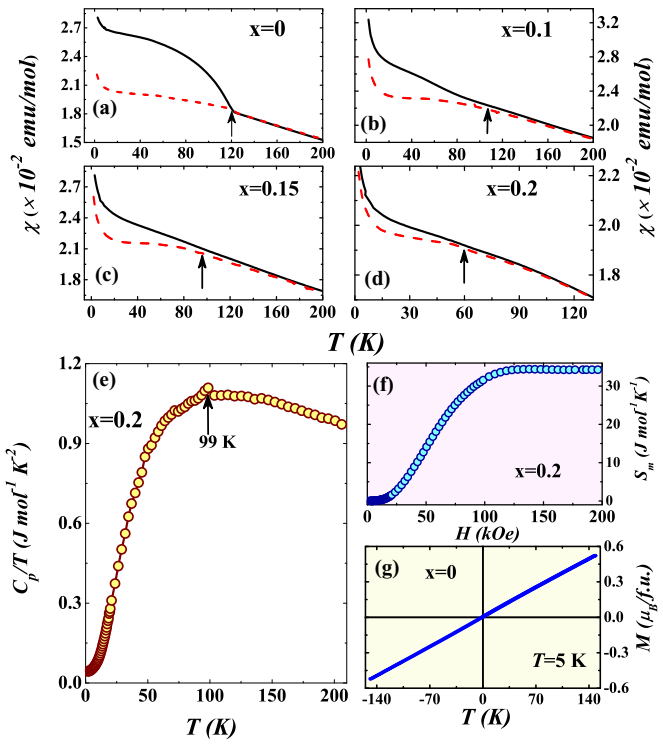

FIG. 4. (a)–(d) The dc magnetic susceptibility χ as a function of temperature for $Eu_{1-x}Sr_xIr_2O_7$ ($x = 0.0$, 0.1, 0.15, and 0.2) at 2 kOe in ZFC and FC protocols. (e) The heat capacity as a function of temperature for the $x = 0.2$ sample. (f) The thermal variation of magnetic entropy and (g) the isothermal magnetization data recorded at 5 K up to an applied field as high as 150 kOe.

is a clear bifurcation between the ZFC and FC χ, and it matches well with literature [4,11]. It is known that several Ir pyrochlores show a long-range all-in-all-out type of magnetic order of Ir close to such thermomagnetic irreversibility (i.e., the bifurcation point of FC and ZFC χ) [11,12]. The point of thermomagnetic irreversibility is often found to be different from the actual ordering temperature; however, it provides a rough indication of the onset of an ordered magnetic phase. We find that the bifurcation is also present in the Sr-substituted samples [Figs. 4(b)–4(d)], and the extent of bifurcation (i.e., $M_{FC} - M_{ZFC}$) diminishes with increasing Sr concentration. The bifurcation point also shifts to lower temperature [indicated by the arrows in Figs. 4(a)–4(d)], and it is found to be $T_{IR} \sim 120$, 107, 97, and 60 K, respectively, for $x = 0.0$, 0.1, 0.15, and 0.2 samples.

The T variation of heat capacity C_p shows a peak at 99 K [Fig. 4(e)] for the $x = 0.2$ sample, which can be ascribed to be the T_N of the sample. This value of T_N obtained from heat capacity is higher than the T_{IR} of the sample. Notably, the feature at T_N is distinct but weak. However, this weak nature is very similar to the data obtained for the single-crystalline sample of $Eu_2Ir_2O_7$ [4]. In order to rule out the possible effect of impurity being responsible for the weak feature in the $C_p(T)$ data, we calculated the magnetic entropy S_m, as depicted in Fig. 4(f) as a function of T. In the absence of a suitable non-magnetic counterpart, we have fitted the high-T data (above T_N) with the Debye heat-capacity model and an electronic part $[C_{nm}(T) = C_{\text{Debye}}(\Theta, T) + \gamma T$, where Θ is the Debye temperature and γ is the Sommerfeld coefficient] and obtained the magnetic part, $C_m = C_p - C_{nm}$. Subsequently, S_m was calculated by using the formula $S_m(T) = \int_0^T (C_m/T')dT'$. We see that $S_m(T)$ tends to saturate above about 100 K, with a value of 34 J/mol K. The expected value of S_m for the low-spin state ($J_{\text{eff}} = \frac{1}{2}$) is much lower (~11 J/mol K). Such a discrepancy may due to a poor estimation of lattice heat capacity or a contribution from the induced moment at the Eu site. In fact, our analysis of the $\chi(T)$ data above 175 K (in the paramagnetic state) indicates a large effective paramagnetic moment ($p_{\text{eff}} = 7.652\,\mu_B$/f.u.), which cannot be accounted for by the low-spin $J_{\text{eff}} = \frac{1}{2}$ state.

Thermomagnetic irreversibility in a material can depend upon various factors such as disorder, magnetic anisotropy, etc. In the present case, although T_{IR} lies below T_N, it signifies the presence of a magnetic state at least below the bifurcation point. The isothermal magnetization curves (M vs H) for all the samples measured at 5 K show linear behavior without any coercivity. As an example, the $M-H$ curve for the $x = 0.0$ sample for $H = \pm 150$ kOe is depicted in Fig. 4(g), which is found to be perfectly linear even at higher fields. This does not support the spin-canted ground state predicted for $Eu_2Ir_2O_7$ [4] and, rather, indicates an antiferromagnetic (AFM) ground state for parent and doped compositions. Such a conclusion is based on the fact that had it been a spin-canted system, there would have been a nonvanishing FM component. This would certainly be reflected in the $M-H$ curve in the form of hysteresis and/or a tendency of saturation of M at higher values of H. On the other hand, a rise in FC χ is observed for all the samples below T_{IR}, which is not generally expected for an AFM system. A very recent experimental work based on torque magnetometry on $Eu_2Ir_2O_7$ indicates the development

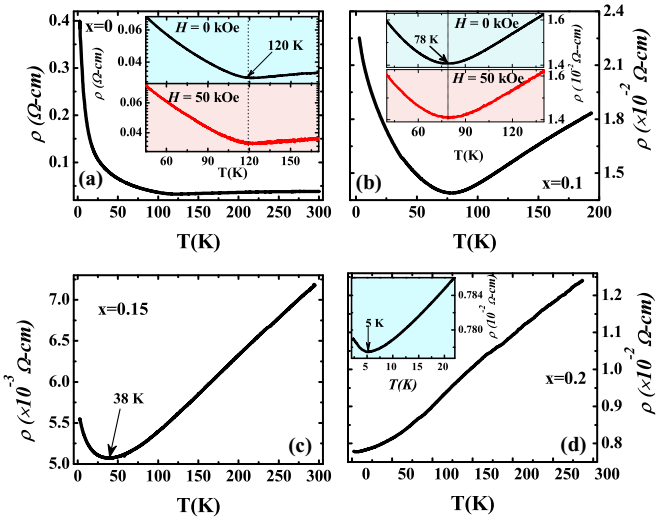

FIG. 5. (a)–(d) The resistivity data as a function of temperature for $Eu_{1-x}Sr_xIr_2O_7$. The insets of (a) and (b) show the metal-insulator transition point at 0 and 50 kOe of applied magnetic fields for the $x = 0.0$ and 0.1 samples, respectively. The inset in (d) shows an enlarged view of the metal-insulator transition for $x = 0.2$.

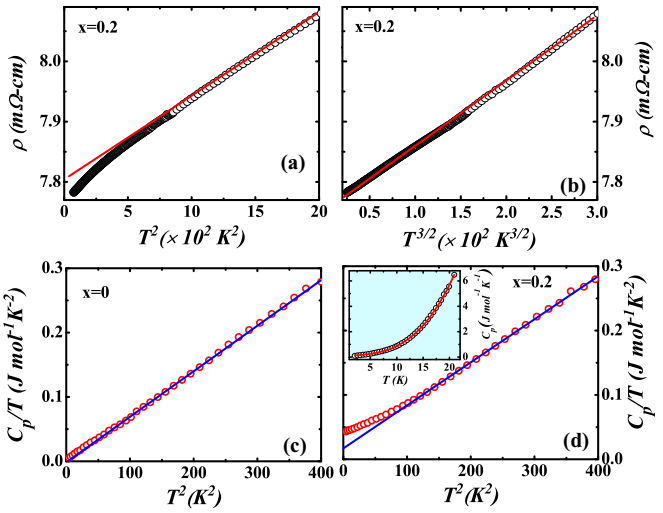

FIG. 7. The variation of low-temperature resistivity as a function of (a) T^2 and (b) $T^{3/2}$ for $x = 0.2$. The solid lines are to guide the eye. (c) and (d) show the variation of C_p/T with T^2 below 20 K for the $x = 0.0$ and 0.2 samples, respectively. The inset shows the low-temperature C_p versus T data along with a fit (solid line) with the relation $C_p = \gamma' T \ln(T_0/T) + \beta T^3$

of a perpendicular magnetization $M_\perp$ of octupolar origin on application of magnetic field in the $a-b$ plane of the crystal [19]. The rise in χ below T_{IR} may be related to this $M_\perp$.

The MI transition in all the samples is probed by dc resistivity studies. The parent sample shows the MI transition at $T_{MI} = 120$ K, below which the sample is insulating. Most interestingly, we found a huge but systematic decrease in T_{MI} with the increase of doping percentage. T_{MI} is found to be 120, 78, 38, and 5 K for the $x = 0.0$, 0.1, 0.15, and 0.2 samples, respectively [Figs. 5(a)–5(d)]. The variation of T_{MI} is found to be almost linear with x [Fig. 6(a)]. Our observation

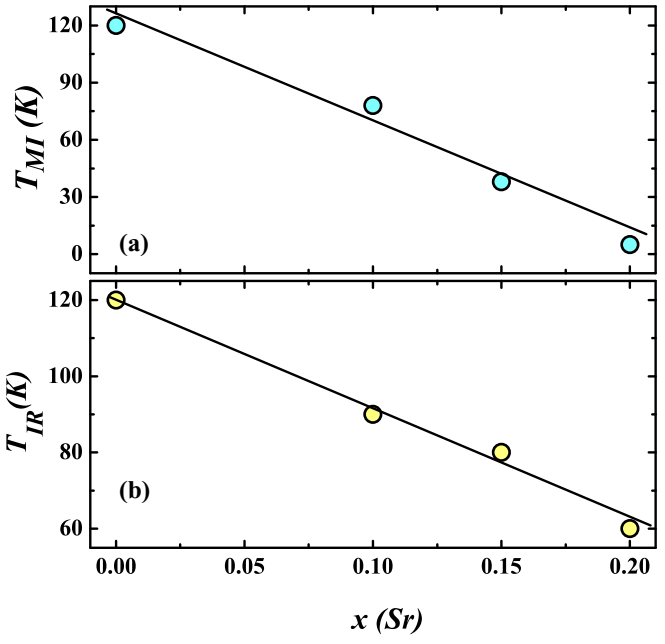

FIG. 6. The variation of (a) T_{MI} and (b) T_{IR} with x.

points to some important facts regarding T_{MI}. First, T_{MI} of the samples does not directly correspond to the magnetic transition temperature. For example, the $x = 0.2$ sample has T_N close to 99 K, while T_{MI} is far below this. This rules out a simple Mott-Slater kind of insulating ground state of the sample. It is to be noted that T_{MI} in $R_2Ir_2O_7$ for different R atoms correspond exactly to their respective T_N [11]. Second, T_{MI} of these samples is found to be insensitive to the applied magnetic field [see the insets of Figs. 5(a) and 5(b) for the $x = 0.0$ and 0.1 samples, respectively], which is in contrast to the scenario of a $3d$ system such as perovskite manganites, where T_{MI} is strongly field dependent. We have also plotted the variation of T_{IR} with x [Fig. 6(b)], and it is clearly seen that T_{IR} for different samples lie well above T_{MI}.

In order to rule out the effect of oxygen off stoichiometry, we annealed a sample piece ($x = 0.0$) in oxygen flow at 800 °C and measured ρ as a function of T. We do not find any noticeable difference in the $\rho(T)$ behavior before and after oxygen annealing (plots not shown). It turns out that oxygen off stoichiometry, even if present to some extent, does not play any role in altering T_{MI}. It is to be noted that for $Nd_2Ir_2O_7$ thin films, oxygen annealing has a marked effect on the physical properties [20].

Considering the fact that the $x = 0.2$ sample shows a MI transition at a fairly low T, we looked carefully at the T dependence of ρ between 7 and 45 K. It is evident that although the system has a metallic character, ρ does not show the clear T^2 variation [Fig. 7(a)] expected for a Fermi liquid. The $\rho(T)$ data can be better described by an empirical $T^{1.5}$ variation, as depicted in Fig. 7(b). Clearly, there is a downward curvature at the low-T side in Fig. 7(a) which is absent in Fig. 7(b). We have also looked at the low-temperature heat-capacity data of the samples, and Figs. 7(c) and 7(d), respectively, show the C_p/T versus T^2 data below 20 K for the $x = 0.0$ and 0.2 samples. We do not see any signature of T_{MI} in the C_p data

for the $x = 0.2$ sample at 5 K. The parent sample shows a linear C_p/T versus T^2 plot which is expected for a crystalline solid as total heat capacity $C_p = \gamma T + \beta T^3$, where γT and βT^3 are, respectively, the electronic and lattice parts. Because this is an AFM insulator, the curve passes through the origin, indicating that there is a negligible electronic contribution to the heat capacity. The spin-wave contribution to C_p for an AFM system also varies as T^3, and it is indistinguishable from the lattice part. On the other hand, for $x = 0.2$, the C_p/T versus T^2 data deviate strongly from the linear behavior below about 12 K. Such an observation is on par with the nonquadratic T dependence of the ρ data at low temperature. The magnetic contribution to C_p is likely to be AFM in both the $x = 0$ and 0.2 samples (as evident from our magnetic measurements), and the deviation from linearity in the C_p/T versus T^2 data is unlikely to be associated with the spin-wave contribution. Also, the spin-wave part is generally negligible below 10 K (T_N is of the order of 100 K). Such an observation clearly demonstrates that the material shows unconventional metallic character. The low-T data can be fitted empirically quite well with the relation $C_p = \gamma' T \ln(T_0/T) + \beta T^3$ [see the inset of Fig. 7(d)], which indicates a logarithmic variation of the density of states at low temperature. In our fitting we find that $T_0 = 17.9$ K, which is much higher than the T_{MI} of the sample.

IV. DISCUSSIONS

The plausible scenario for the metallicity in the Sr-substituted materials is connected to hole doping, which makes the sample mixed valent with the presence of both Ir^{4+} and Ir^{5+} ions. It is well established that SOC is lower in the case of Ir^{5+} ($5d^4$) compared to Ir^{4+} ($5d^5$) [21]. In a recent work by Bhowal *et al.* [22] based on density-functional-based calculations, it is found that for double-perovskite-based d^4 iridates, the electronic bandwidth W of the t_{2g} level is higher. In the event of $W \gtrsim$ SOC, there can be overlap of the $J_{\text{eff}} = 1/2$ and $J_{\text{eff}} = 3/2$ bands. If $W \gtrsim$ SOC and U, partially filled Hubbard bands can exist even in the presence of U. Further, hybridization between the d^5 and d^4 states can lead to additional band widening in the doped samples [Fig. 1(b)]. Such effects can together facilitate band overlapping, leading to a more metallic behavior in the Sr-doped samples.

The transitions at T_{MI} for the doped (as well as the parent) compositions are found to be continuous (unlike pure Mott transition) and do not correspond grossly to T_N. Therefore, Anderson localization-type phenomenon may be the prevalent cause for the insulating ground state even for the highest doped sample. Considering the presence of finite electronic correlation, the transition may aptly be described as an Anderson-Mott type [23].

One of the important observations is the non-Fermi liquid (NFL) behavior of the highest doped sample ($x = 0.2$) as evident from both ρ and C_p studies. The sample is already in the magnetically ordered state, and proximity to a quantum critical point can be ruled out for NFL behavior. In addition, it is unlikely for quantum fluctuation to dominate over thermal fluctuation at 10 K (the temperature below which the NFL state is observed). Despite the metallic nature down to 5 K in $x = 0.2$, the absolute value of ρ is high. The Mott-Ioffe-Regel (MIR) value of the minimum conductivity of a metal is given by $\sigma_{\min} = 0.03e^2/\hbar r_{nn}$ [24], where r_{nn} is the nearest-neighbor atomic distance, and for a pyrochlore structure it is $(a_c/4)\sqrt{2}$. For the $x = 0.2$ sample, the maximum metallic resistivity $\rho_{\max}$ (the reciprocal of $\sigma_{\min}$) turns out to be 4.8 mΩ cm, which is lower than the experimentally observed ρ even at 5 K without the signature of *resistivity saturation*. Such *bad metals* violating the MIR rule are not uncommon among correlated electron systems, including high-T_C cuprates, ruthenates, nickelates, and doped fullerides [25–28], and a mutual interplay between disorder and correlation has often been attributed to the effect. Notably, the MIR formula had been primarily derived for disordered solids (so-called bad metals) and is equally applicable for a polycrystalline sample with grain and grain boundaries [29].

The deviation from an FL ground state and the violation of the MIR rule can be thought to be intercorrelated [25]; however, they are not universally supported by the experimental observations [30]. There are examples of bad metals among ruthenates which show FL characteristics [26,31]. The metallic NFL behavior is conjectured theoretically in a correlated disordered system prior to an Anderson-Mott-type MI transition [32]. The situation might be more exciting in these doped $Eu_2Ir_2O_7$ compositions, in which SOC is important in addition to U. The presence of the NFL state in a correlated electron system with SOC (such as a pyrochlore iridate) has been argued by Moon *et al.* [16]. In our study, the NFL behavior is observed only in the doped composition, and this may be an indication of the role of disorder in the observed deviation from the FL. In fact, NFL behavior in the metallic phase of $SrIrO_3$ thin films is attributed to the strain-induced disorder [33]. The effect of disorder is well documented in Kondo lattice systems, where a distribution of the Kondo temperature can lead to an NFL ground state [34]. Since SOC in Ir^{4+} is higher than in the Ir^{5+} ion [21], one can have a spatial distribution of SOC over the doped sample, which can be held responsible for the NFL behavior.

Summarizing, we find a systematic change in the metal-insulator transition temperature on hole doping in $Eu_2Ir_2O_7$. From our sample characterization by atomic force microscopy, these polycrystalline ceramics samples are found to be made up of closely packed grains without much void space. The careful analysis of the x-ray diffraction pattern also indicates full site occupancy of the atoms at the crystallographic positions. The oxygen off stoichiometry can also be ruled out for the change in T_{MI}, as additional oxygen annealing has little or no effect on the metal-insulator transition. The x-ray photoemission spectra indicate the clear presence of Ir^{5+}, which plays an important role in determining ground-state electronic and magnetic properties. We find that the system violates the Mott-Ioffe-Regel value of minimum conductivity for disordered bad metals, which indicates that the strong electronic correlation in the presence of disorder is operating here. The most important observation is the NFL behavior in the case of the $x = 0.2$ sample. Such a deviation from the regular FL ground state cannot be ascribed to the polycrystalline nature of the sample (grains, grain boundaries, or other dislocations), as it is absent in the parent compound. We opine that the random distribution of Ir^{4+} and Ir^{5+} ions in the sample provides a spatial variation of spin-orbit-coupling strength, which in turn provides multiple renormalization coefficients

for the interacting electrons to be mapped on a simple noninteracting Drude-Sommerfeld model to form the FL state. Such multiplicity as a whole breaks the FL state, and an NFL state emerges. The NFL state thus indirectly depends upon the disorder at the atomic level, but not on the bulk disorder. It resembles the Kondo disorder model of some heavy-fermion alloys showing NFL behavior, where a distribution Kondo temperature (compared to the SOC energy scale in the present case) breaks the FL state.

Note added in proof: Recently, we became aware of the theoretical work by Shinaoka *et al*. [35], which predicts non-Fermi-liquid behavior in the electron- or hole-doped $Y_2Ir_2O_7$ originating from long-lived quasi-spin-moments induced by nearly flat bands.

ACKNOWLEDGMENTS

The authors would like to thank I. Dasgupta and S. Bhowal (IACS) for useful discussions. K. G. Suresh (IIT Bombay) and S. Chatterjee (UGC-DAE-CSR, Kolkata) are thankfully acknowledged for different measurements. A.B. wishes to thank the DST-INSPIRE program for the research assistance. J.S. wishes to acknowledge EU's Horizon 2020 research and innovation program.

[1] B. J. Kim, H. Jin, S. J. Moon, J.-Y. Kim, B.-G. Park, C. S. Leem, J. Yu, T. W. Noh, C. Kim, S.-J. Oh, J.-H. Park, V. Durairaj, G. Cao, and E. Rotenberg, Phys. Rev. Lett. **101**, 076402 (2008).
[2] B. J. Kim, H. Ohsumi, T. Komesu, S. Sakai, T. Morita, H. Takagi, and T. H. Arima, Science **323**, 1329 (2009).
[3] K. Matsuhira, M. Wakeshima, R. Nakanishi, T. Yamada, A. Nakamura, W. Kawano, S. Takagi, and Y. Hinatsu, J. Phys. Soc. Jpn. **76**, 043706 (2007).
[4] J. J. Ishikawa, E. C. T. OFarrell, and S. Nakatsuji, Phys. Rev. B **85**, 245109 (2012).
[5] S. T. Bramwell and M. J. P. Gingras, Science **294**, 1495 (2001).
[6] L. D. C. Jaubert and P. C. W. Holdsworth, Nat. Phys. **5**, 258 (2009); S. Ladak, D. E. Read, G. K. Perkins, L. F. Cohen, and W. R. Branford, *ibid.* **6**, 359 (2010).
[7] D. Pesin and L. Balents, Nat. Phys. **6**, 376 (2010).
[8] B.-J. Yang and Y. B. Kim, Phys. Rev. B **82**, 085111 (2010).
[9] X. Wan, A. M. Turner, A. Vishwanath, and S. Y. Savrasov, Phys. Rev. B **83**, 205101 (2011).
[10] A. B. Sushkov, J. B. Hofmann, G. S. Jenkins, J. Ishikawa, S. Nakatsuji, S. D. Sarma, and H. D. Drew, Phys. Rev. B **92**, 241108(R) (2015).
[11] K. Matsuhira, M. Wakeshima, Y. Hinatsu, and S. Takagi, J. Phys. Soc. Jpn. **80**, 094701 (2011).
[12] K. Tomiyasu, K. Matsuhira, K. Iwasa, M. Watahiki, S. Takagi, M. Wakeshima, Y. Hinatsu, M. Yokoyama, K. Ohoyama, and K. Yamada, J. Phys. Soc. Jpn. **81**, 034709 (2012).
[13] S. M. Disseler, C. Dhital, A. Amato, S. R. Giblin, C. de la Cruz, S. D. Wilson, and M. J. Graf, Phys. Rev. B **86**, 014428 (2012).
[14] H. Sagayama, D. Uematsu, T. Arima, K. Sugimoto, J. J. Ishikawa, E. O'Farrell, and S. Nakatsuji, Phys. Rev. B **87**, 100403(R) (2013).
[15] K. Ueda, J. Fujioka, Y. Takahashi, T. Suzuki, S. Ishiwata, Y. Taguchi, and Y. Tokura, Phys. Rev. Lett. **109**, 136402 (2012).
[16] E.-G. Moon, C. Xu, Y. B. Kim, and L. Balents, Phys. Rev. Lett. **111**, 206401 (2013).
[17] FULLPROF, https://www.ill.eu/sites/fullprof/
[18] T. Otsubo, S. Takase, and Y. Shimizu, ECS Trans. **3**, 263 (2006).
[19] T. Liang, T. H. Hsieh, J. J. Ishikawa, S. Nakatsuji, L. Fu, and N. P. Ong, Nat. Phys. **13**, 599 (2017).
[20] J. C. Gallagher, B. D. Esser, R. Morrow, S. R. Dunsiger, R. E. A. Williams, P. M. Woodward, D. W. McComb, and F. Y. Yang, Sci. Rep. **6**, 22282 (2016).
[21] D. Khomskii, *Transition Metal Compounds* (Cambridge University Press, Cambridge, 2014).
[22] S. Bhowal, S. Baidya, I. Dasgupta, and T. Saha-Dasgupta, Phys. Rev. B **92**, 121113(R) (2015).
[23] D. Belitz and T. R. Kirkpatrick, Rev. Mod. Phys. **66**, 261 (1994).
[24] N. F. Mott, *Metal-Insulator Transitions*, 2nd ed. (Taylor and Francis, London, 1974).
[25] V. J. Emery and S. A. Kivelson, Phys. Rev. Lett. **74**, 3253 (1995).
[26] G. Cao, W. H. Song, Y. P. Sun, and X. N. Lin, Solid State Commun. **131**, 331 (2004).
[27] O. Gunnarsson, M. Calandra, and J. E. Han, Rev. Mod. Phys. **75**, 1085 (2003).
[28] E. Mikheev, A. J. Hauser, B. Himmetoglu, N. E. Moreno, A. Janotti, C. G. Van de Walle, and S. Stemmer, Sci. Adv. **1**, e1500797 (2015).
[29] P. P. Edwards, M. T. J. Lodge, F. Hensel, and R. Redmer, Philos. Trans. R. Soc. London, Ser. A **368**, 941 (2010).
[30] N. E. Hussey, K. Takenaka, and H. Takagi, Philos. Mag. **84**, 2847 (2004).
[31] A. P. Mackenzie, S. R. Julian, A. J. Diver, G. J. McMullan, M. P. Ray, G. G. Lonzarich, Y. Maeno, S. Nishizaki, and T. Fujita, Phys. Rev. Lett. **76**, 3786 (1996).
[32] V. Dobrosavljević and G. Kotliar, Phys. Rev. Lett. **78**, 3943 (1997).
[33] A. Biswas, K.-S. Kim, and Y. H. Jeong, J. Appl. Phys. **117**, 115304 (2015).
[34] E. Miranda, V. Dobrosavljević, and G. Kotliar, Phys. Rev. Lett. **78**, 290 (1997).
[35] H. Shinaoka, S. Hoshino, M. Troyer, and P. Werner, Phys. Rev. Lett. **115**, 156401 (2015).